Taylor & Francis
Taylor & Francis Group

A Review on Spider Silk Adhesion

Vasav Sahni[1], Todd A. Blackledge[2], and Ali Dhinojwala[1]
[1]Department of Polymer Science, The University of Akron, Akron, Ohio, USA
[2]Department of Biology and Integrated Bioscience Program, The University of Akron, Akron, Ohio, USA

Spiders employ clever behavioral strategies combined with almost invisible custom-made adhesive silk fibers to spin prey capture webs. The adhesives used in these webs evolved over millions of years into a class of natural materials with outstanding properties. Here, we review how spiders use different adhesives to capture prey. We show how spiders take advantage of the elasticity of both the capture silk and the glue to enhance adhesive forces, thereby providing important insights in designing new synthetic adhesives.

1. INTRODUCTION

Bonding different materials together by means of an adhesive may appear mundane to most people. In reality, a great deal of science and technology is involved in this simple action of bonding. Adhesive manufacturing continues to grow due to the diversity of substrates and the continuous introduction of new chemistry and processes. However, long before human industry, nature evolved many well-designed adhesives for locomotion, defense, and prey capture. Geckos use micron-sized hairs as dry reversible adhesives for locomotion [1]. Mussels secrete specialized proteins to stick to rocks under water

[2]. Spiders employ multiple kinds of silk fibers in different web-building strategies to capture prey [3]. In this review, we discuss some fascinating examples of adhesives used by spiders in the hope to stimulate the use of these principles in designing new adhesives.

2. SPIDER WEBS

Webs evolved early in the evolutionary history of the world's 41,000+ species of spiders [4]. Webs provide spiders with the means to trap their food, a place to shelter, and even an arena in which they mate. Webs are assembled from several unique types of silks that function together as integrated units helping to make spiders highly efficient and successful predators. Almost all of the spider families have web-building members [5]. Their web designs and prey-capturing strategies, as shown in Fig. 1, range from two-dimensional sheets to three-dimensional tangles to the wheel-like orb web [6]. The spider's web is primarily a trap, mostly for insects. Webs first stop or slow prey and then transmit the location of the trapped insects to the waiting spiders. This represents a formidable challenge because of the high kinetic energy of prey, especially flying insects, and spiders must react quickly to prey to prevent insects from escaping. This places a premium on the adhesive capabilities of spider silks.

Spiders evolved many interesting and innovative strategies that use silk to capture prey over their ~400 million year history [6]. Almost all of these strategies involved spiders spinning multiple kinds of silk threads "custom-made" for different functions within webs. Given the immense variation in web architecture among spiders, it is no surprise that different types of silks evolved unique sets of material properties and that silk performance can vary immensely across different species [7].

Silkworm silk is an important and high-priced textile commodity used for thousands of years [8]. In contrast, spider silks have yet to be utilized on a large scale despite their desirable qualities because of the difficulty of "farming" spiders. Only rather recently have we begun to realize that spider silks can inspire us to make high-performance synthetic mimics for myriads of applications. Much research is underway to characterize the protein "tool-box" that the spiders use to spin these "intelligent" biomaterial fibers [9] and to express these proteins in more conveniently farmed organisms like goats, bamboo trees, bacteria, and silkworms [10]. The main aim of this review article is to discuss the adhesion of viscid and cribellar capture silks in orb webs. However, the orb is an intermediate "stepping stone" in the evolution of web spinning, facilitating new innovations in
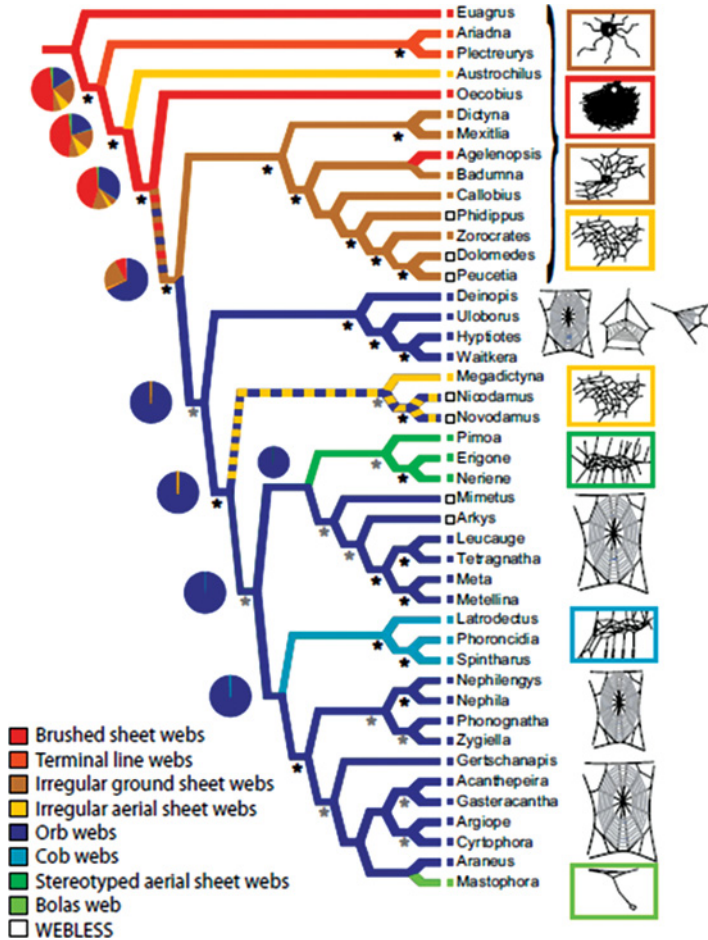
FIGURE 1 Different kinds of prey capturing strategies. Optimization of spider web architectures on an evolutionary tree of spiders. Adapted from [6] with permission (color figure provided online).

silks and webs. Thus, we first introduce a few of the diverse silks and web spinning strategies of spiders, as shown in Fig. 1 [5], to provide context.

2.1. Bolas Spiders

Bolas spiders (*Mastophora* spp.) are atypical orb-weaving spiders that do not weave a typical orb-web. Instead, they hunt mostly male moths

FIGURE 2 Bolas Spider. A bolas spider with its web — a gluey blob at the end of a single silk line that it swings to catch its moth prey. Adapted from http://nathistoc.bio.uci.edu/spiders/Mastophora.htm (color figure provided online).

by using a sticky blob at the end of a silk fiber, known as a "bolas" (Fig. 2). By swinging the bolas at flying male moths or moth flies in their vicinity, these spiders snag their prey much like a fisherman snagging a fish on a hook. The female spiders provide a remarkable example of aggressive mimicry when they release chemicals similar to the sex attractants that are produced by female moths to attract the male moths [11,12]. The gluey bolas silk evolved from the viscid silk of normal orb-weavers but overcomes a serious challenge—the scales of moths and butterflies rub off easily, allowing these insects to escape most orb webs. The bolas glue, in contrast, soaks through the scales and adheres to the underlying cuticle of these challenging preys.

2.2. Brown Recluse Spiders

Famed for their hemolytic venom [13], which can cause necrotic lesions, these spiders (*Loxosceles* spp.) also spin silk retreats underneath objects. These retreats usually consist of two sheets of silk threads with a space between them for the spider and a tangle of loose threads outside the sheets. The lower sheet is in contact with the substrate while the upper sheet, attached to the underside of objects, has a small hole which the spider uses to exit. While the general structure of these webs is characteristic of the behaviors of many groups of "primitive" spiders that mostly lack adhesive silk, the silk produced by brown recluse spiders is noteworthy. These sheets are composed
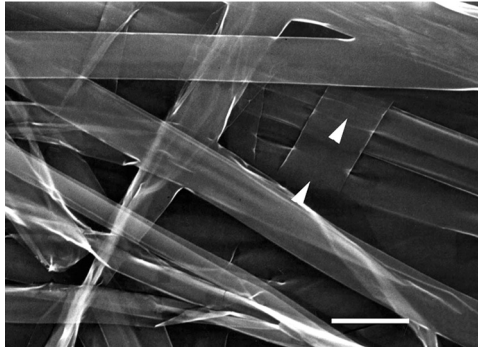
FIGURE 3 Ribbon silk. Figure shows an SEM image of the major ampullate silk spun by female *L. laeta*. The silk is unique in its highly anisotropic shape, compared with the relatively cylindrical silk of most other spiders. Arrows point towards the plaque of adhesion between ribbons. Scale bar is 10 μm. It is adapted from [15] with permission of the Royal Society London.

of a maze of ribbon-like, rather than cylindrical, silk anchored to surfaces by thousands of very fine threads (Fig. 3). The silk ribbons adhere very well to each other and the whole network is highly elastic with ribbons capable of extending up to twice their length with low hysteresis [14,15].

2.3. Black Widow Cobwebs

The cobweb of the black widow spider (*Latrodectus hesperus*) has a three-dimensional structure comprised of two distinct prey capture surfaces, a catching sheet and supporting threads that can physically entangle flying insects and sticky gum-footed threads that target walking prey. Sticky gum-footed threads are vertical and extend from the substrate to the catching sheet of the cobweb. They are easily detached from the substratum when disturbed by walking prey. Glue droplets at the bottom of the sticky gum-footed threads adhere to the prey. Typically, one sticky gum-footed thread contains four fibers of silk. During web construction, the spider marks suspension sites on the scaffolding silk prior to laying any gum-foot. This site becomes the top, or vertex, of the gumfoot thread. At the vertex, a cement material serves to mechanically link the scaffolding and sticky gum-footed threads. During web construction, the widow spider spins the first pair of threads from the vertex to the substrate. The spider then attaches the sticky gum-footed thread to the substrate and begins spinning the second pair of threads as the spider crawls back to the
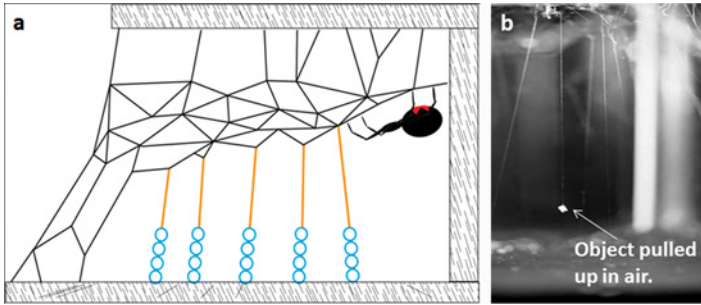
FIGURE 4 Cob webs. (a) A schematic of a cob-web; (b) Cob webs can capture flying prey as well as walking insects. When a walking insect contacts a sticky gum-footed thread, it quickly detaches from the substrate and yanks the insect into the air. Figure shows a simulation of this using a white mass instead of an actual insect. It is adapted from [16] with permission of Springer (color figure provided online).

vertex. Nearly simultaneously, the lower sticky gum-footed threads are coated with viscid droplets. The viscid droplets extend 0.5 to 2 cm on the lower portion of the gumfoot. The spider also cuts the first pair of threads midway back to the vertex, allowing the final sticky gum-footed thread to be pulled under tension. When detached, the sticky gum-footed threads quickly yank the prey upwards. Small prey become suspended helplessly in the air after detaching a single gum-foot thread (Fig. 4). Larger prey items are captured with several gum-foot threads [16,17] and by active attack. The attack behavior of widow spiders is also noteworthy because they utilize a liquid that is secreted from a unique, enlarged set of aggregate glands that they fling onto prey. This glue appears to harden rapidly over several seconds.

2.4. Orb-Weaving Spiders

These spiders, like most spiders, produce many types of silk, typically seven, each of which has specific properties that appear to be optimized to perform key functional roles. Dragline silk, produced by the major ampullate glands, makes the spokes (or radii) of the wheel-like orb web (Fig. 5). The spiders also produce minor ampullate silk to accompany the dragline silk in the web, as well as flagelliform silk that forms the core filaments of the orb web's capture threads. The web threads are anchored to the vegetation and affixed to one another by silk cement originating in the pyriform glands. The eggs are encased in very fine silk filaments from the tubuliform or

FIGURE 5 Orb-web. Figure shows a typical orb-web (color figure provided online).

cylindriform and one type of aciniform gland, while another type of aciniform filament is used for a multitude of other purposes such as strengthening the cement matrix. The orb-weavers use two kinds of capture threads to capture prey: either cribellar silk or viscid silk [18,19]. Cribellate capture silk is relatively ancient and utilized by many types of web-spinning spiders while viscid silk evolved more recently and is used by most modern orb-weaving spiders [20]. Understanding the structure, morphology, and adhesive mechanism of both of these kinds of glues is the main goal of this article.

2.4.1. Cribellar Silk

The cribellate spiders have a unique silk producing structure called a cribellum, just in front of the spinnerets. This broad plate is set firmly in the spider's abdominal cuticle and is covered with thousands of tiny spigots [21]. This cribellum plate produces swaths of the finest gossamer silk, which, when drawn out by combs on the spider's legs, come out hackled. Charge is imparted to these drying filaments while

combing, causing these nanofibers to repel each other and puff out to form a nanoscale, wool-like yarn. The resulting nano-filamentous mesh adheres to, and often totally covers, a pair of much thicker (micron-sized) supporting fibers issuing from spigots on the main spinnerets [22]. Some spiders further reinforce this multi-fiber assembly by imparting crimped, spring-like fibers from yet another set of spigots, which pull up tight by the now rather complex, composite fiber [23]. Hackling cribellum silk is expensive for the spider, in terms of the time it takes to produce and the energy it expends. This is very evident from the fact that a cribellate spider moving along and laying a thread in its web is slow and also that its two hind-legs rapidly comb away the nanofibers [24].

A completed cribellar thread often forms a series of regular puffs (Fig. 6a). Adhesiveness of this thread depends on the density of the nanofibers that form its surface and is modified by the dimensions of the puffs and the manner in which a spider loops and folds a finished thread [25,26]. There are approximately 3,606 species that spin cribellar silk threads. Of these, 11 species produce primitive, cylindrical, non-noded nanofibers and the rest produce nanofibers with regularly spaced nodes [27] (Figs. 6b and c). A couple of different adhesion mechanisms account for the adhesiveness of these cribellar threads. Indubitably, mechanical interlocking provides one mechanism for capturing insects as the nanofibers on the thread's surface snag an
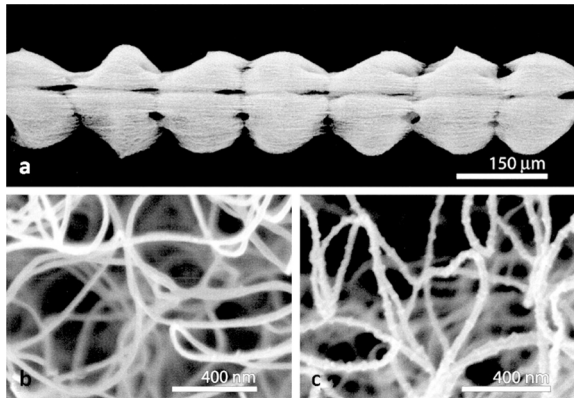

FIGURE 6 Cribellar Silk. (a) A completed cribellar thread often forms a series of regularly spaced puffs that are brushed into place by the spider's legs. The surface of these threads is made up of thousands of nanofibers. These nanofibers can be either (b) non-noded or (c) noded. It is adapted from [27] with permission of John wiley & sons., Ltd.

insect's setae and retain them just as a Velcro[TM] fastener works [28]. Interestingly, this hierarchical structure also adheres to smooth surfaces such as glass and graphite just like the gecko toe pad. Electrostatic attraction, van der Waals forces, and hygroscopic (capillary) forces were all hypothesized to account for cribellar silks' adhesiveness and tested. Quantifying adhesion of these micron-sized threads involves placing the thread between two legs of a cardboard mount, bringing it in contact with a solid substrate, and then detaching the thread at a controlled rate such that the force exerted just before pull-off is taken as the force of adhesion [29] (see Fig. 11c, inset). No significant difference was found in the force of adhesion values when cribellar threads were adhered to substrates of very similar texture but different dielectric constants, which ruled out electrostatic adhesion [30]. This just left two possible mechanisms to explain adhesion: van der Waals forces and hygroscopic adhesion.

Subsequent studies conducted by Hawthorn and Opell [31] repeated these tests in environments with different humidity to determine the possible role of water for adhesion of cribellar threads. Again, the presence or absence of humidity did not affect the adhesion of primitive cribellar threads (non-noded nanofibers). However, evolutionarily derived cribellar threads (noded nanofibers) adhered better at higher values of humidity. Based on these observations, Hawthorn and Opell concluded that primitive cribellar threads likely use van der Waals forces to adhere to smooth surfaces, whereas, derived cribellar threads can also employ capillary forces. This hypothesis was then tested by modeling the van der Waal forces and capillary forces as follows:

$$\mathbf{F}_{\mathrm{vdW}} = \frac{AR}{6D^2} \quad \text{and} \quad \mathbf{F}_{\mathrm{C}} = 4\pi R \lambda_{\mathrm{L}} \cos\theta,$$

where the subscripts vdW, C, and L mean van der Waal forces, capillary forces, and liquid (water), respectively. A is the Hamaker constant, taken to be $45 * 10^{-21}$ J, R is the radius of the sphere (for noded nanofibers, the radius of a node of cribellar nanofibers and for cylindrical nanofibers, the radius of a cribellar nanofiber), and D is the distance between the sphere and the substrate where van der Waals forces become significant. λ_{L} is the surface tension of water $(76\,\mathrm{mJ\,m^2})$ and θ is the angle of contact between the water and the substrate. The number of contact points per unit area was determined for both primitive as well as derived cribellar threads and the forces were multiplied by the total number of points in contact. A good agreement was found between the experimental and the theoretical results and,

hence, it was concluded that primitive cribellar threads use van der Waals forces whilst the derived cribellar threads employ hygroscopic forces to accomplish adhesion [31]. Surprisingly, in this model, the stretching of the axial fibers was not taken into account when determining the causes of the adhesion exerted by these threads on flat substrates. Also, it was assumed that all the points of contact were contributing equally to the overall adhesion force exerted by the thread, which was later shown to be incorrect (Section 2.4.3).

2.4.2. Viscid Silk

Cribellar nanofibers were replaced in webs by the evolution of aqueous-based, chemically adhesive glue in modern orb-weavers (*Aranoidea*) [32]. This transition to aqueous glue is associated with a dramatic increase in diversity of *Araneoidea* compared with its cribellate sister lineage *Deinopoidea* and can be attributed to the "success" of glue and the composite viscid silk thread over the cribellar threads [6]. Orb-weavers rely upon a combination of strength and stiffness from the dragline silk and stretchiness of the capture spiral to absorb the kinetic energy of flying insects that impact webs [33]. The adhesiveness of the capture spiral then retains insects long enough to be located and captured by spiders [34]. The strength, stretchiness, and stickiness of viscid silk capture threads have a synergistic effect which outperforms cribellar threads in capturing prey, and hence the resulting increase in diversity of *Araneoidea* as compared with *Deinopoidea* [35].

The viscid threads of orb-weaving spiders consist of two soft, but highly extensible, axial fibers surrounded by aqueous adhesive glue (Fig. 7a). These threads are produced from triads of spigots that lie on the left and right posterior spinnerets. Each triad is composed of a gland that produces an axial fiber (flagelliform gland), two glands that secrete the glue (aggregate gland), and their respective spigots. The spigot from the fiber gland is arranged between the spigots of the glue glands such that glue and fibers are simultaneously extruded (Fig. 7b) [6]. At first the glue covers the fibers evenly but it soon spontaneously forms into a series of more or less regularly distributed droplets due to Rayleigh instability [5,36]. A number of studies have chemically characterized the components of these glue droplets. Using NMR, the water soluble fraction of this silk was found to contain a concentrated solution of hygroscopic components related to neurotransmitters like GAB-amide, N-acetyltaurine, choline, betaine, isethionic acid, cysteic acid, lysine, serine, potassium nitrate, potassium dihydrogenphosphate, and pyrrolidone. The water soluble fraction, however, does not contain any polymer. The concentration of salt present
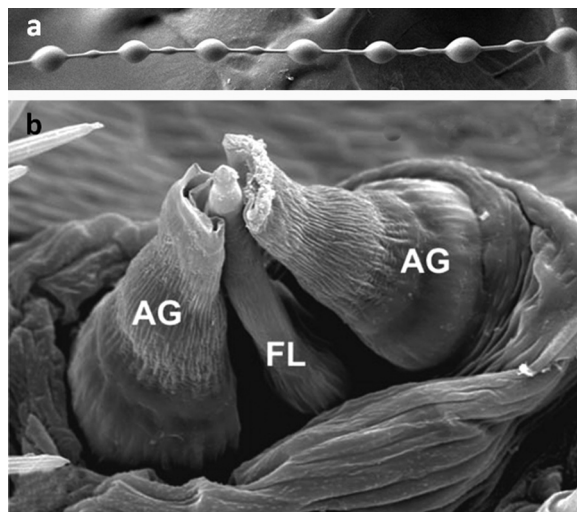
FIGURE 7 Viscid silk. (a) SEM (JEOL) image of a completed viscid capture silk spun by *Lariniodes cornutus*. This kind of capture silk is spun using a triad of spigots. Axial silk is spun in the flagelliform (FL) gland after which it is coated with aqueous glue produced in the aggregate (AG) glands as shown in (b). Figure 7b is adapted from [6] with permission.

determines the amount of water uptake by this system. Also, the high concentration of salts gives a vapor pressure very close to ambient humidity values prevalent at the habitat of these spiders. Also, the compounds do not react electrostatically with the anionic glycoprotein because they are either positively charged organic amines, zwitterions, or anions of very strong acids—sulphonates. Moreover, these salts do not crystallize over a wide range of vapor pressures, unlike salts like NaCl [35].

The polymer fraction of the glue drops was dissolved in trypsin and was analyzed for neutral and amino sugars using the Masamune-Sakamoto method and amino acid analyzer, respectively. The results indicated the presence of galactosamine, mannose, galactose, glucosamine, fucose, and glucose [37]. When the cylindrical glue coating applied by the spider breaks into droplets, these compounds assume a "drop within a drop" like morphology. Optical imaging showed that the "inner drop" is fibrous and it was hypothesized that the glycoproteins lie there. Staining the capture silk threads with fluorescent lectin molecules confirmed that the N-acetylgalactosamine, and, hence, the glycoproteins, are present in the "inner" drops. It was hypothesized that the glycoproteins, being the only component in the glue drop with

long branches, can act as glue *sensu strictu*. Sliding the thread between two smooth surfaces resulted in uncoiling and stretching of the fibers in the inner drop after the viscous liquid had dried out, which supported the hypothesis that the glycoproteins do, indeed, act as the glue [38]. When these threads were exposed to osmic acid, their surface stained black suggesting the presence of fatty compounds in a "superficial" layer on these threads (the NMR of the water-soluble fraction showed highly saturated fatty acids). Visual observations of a slice of the cross-sections of these droplets also showed the presence of a dense superficial layer. Based on these observations, a two-phase model was hypothesized for these droplets in which the central dense region was the glycoprotein and the surrounding transparent region was the viscous coat [39].

However, due to recent visual observations and calculations of the relative sizes of the "inner droplet" and the extent of stretching of the whole droplet when detaching from a surface, it was hypothesized that the glue drops assume a three-phase model instead. These three regions are a small central, opaque anchoring granule, a larger surrounding, transparent glycoprotein glue region, and a more fluid outer covering that extends onto inter-droplet regions (Fig. 8). This organization would allow droplets to generate adhesion, elongate under a load, transfer force to the axial fibers, and resist slippage on the axial fibers [40].

Yet, the role of water in the aqueous material and the composition of the capture threads remained to be determined. These questions were answered using solution state NMR experiments on silk with
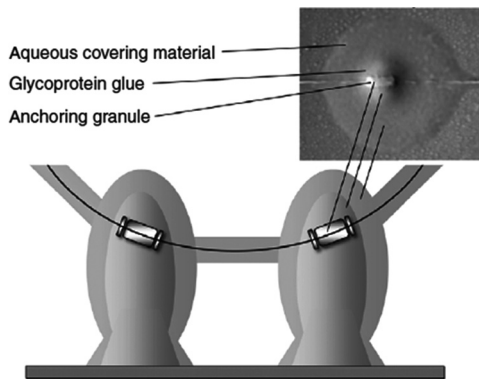

FIGURE 8 Structure of the glue droplet. a) Figure shows a schematic of the hypothesized three-phase model of the glue droplets. It is adapted from [40] with permission.

the idea that mobile molecules in solids yield high-resolution spectra. Peaks corresponding to the components of the viscid coating, along with the observation of full Nuclear Overhauser effect, indicated that the coating is mobile. These peaks disappeared and reappeared on dehydrating and subsequently rehydrating the webs. When these webs were washed with D_2O and dried, subsequent NMR showed low signals consistent with protein. These signals were later associated with the glycoproteins. The crucial observation here was that, in the presence of water, the viscid capture silk was partly mobile on the NMR timescale. The intensity of this capture web spectrum is roughly comparable with that of a similar quantity of a small soluble protein and suggests that a large fraction of the web is visible in these spectra and is, therefore, mobile. Capture fibers, therefore, act like an elastomer that is well above its glass transition temperature and has very low crystallinity. The loss of NMR signals when the silk dried showed that the water acts as a plasticizer for the silk. The difference in composition of radial silk compared with capture silk is evidenced by its lack of significant NMR signals in water. Water, thus, plays a huge role in the capture silk elasticity [41].

2.4.3. Adhesion of Cribellar and Viscid Threads

Differences in the dimensions of the adhesive material and the mechanical properties of the underlying axial fibers suggest that cribellar and viscous capture threads function differently in achieving adhesion values per volume of thread material. These differences include the scale at which a thread interacts with a surface, the efficiency with which adhesive forces are transferred to the thread's axial fibers, and the ability of a thread span to recruit adhesion from interior regions of contact. Cribellar threads interact *via* nanofibers that are around 20 nm in diameter. Nanofibers of evolutionarily derived cribellar threads have regularly spaced 35 mm diameter nodes that establish around 170 contact points per μm^2. In contrast, viscous threads typically have 30 or fewer droplets per mm and mean droplet dimensions of 10 μm or greater. Thus, cribellar thread generates adhesion at many small, diffuse points of contact, whereas viscous thread generates adhesion at a few large points of contact. Due to the diffuse nature of the contact established by the cribellar threads, the adhesion generated at these points is not effectively summed and transferred to the axial fiber. Viscous thread, on the other hand, generates adhesion using much fewer collinear droplets that effectively transfer this force to the axial fibers. Useful adhesion is generated only at the outer edges of contact of a cribellar thread with a surface, based on the observation that cribellar threads do not exhibit

any significant difference in the force values when adhered to plates of different widths. The limited softness and extensibility of cribellar axial fibers could explain this effect. In contrast, the greater extensibility of viscous threads, and of the viscoelastic droplets, produces a highly extensible system capable of transferring more force along the thread's axial lines, hence, recruiting more adhesion by inner droplets and is termed the "suspension bridge mechanism" (Fig. 9) [42].

Most studies trying to quantify adhesion of silk threads bring a single thread in contact with a smooth substrate, and then retract it such that the force registered just before the thread releases contact with the substrate is called the adhesive force of the thread. One major shortcoming of this approach is the absence of any information on the mechanics of the glue drops. This is partly because of the inability of researchers to probe the glue drops and partly because previous studies involved measuring the force required to separate (pull-off) single capture threads from a surface. Force at pull-off depends on the mechanics of both axial silk and glue drops and, hence, the contribution of the glue is not directly inferable. Also, because of the nature of this measure, it depends on parameters like length of the thread and width of the substrate. Any intra-species or inter-species variation in adhesion cannot be understood by using force values if these studies have been performed in different laboratories (under different
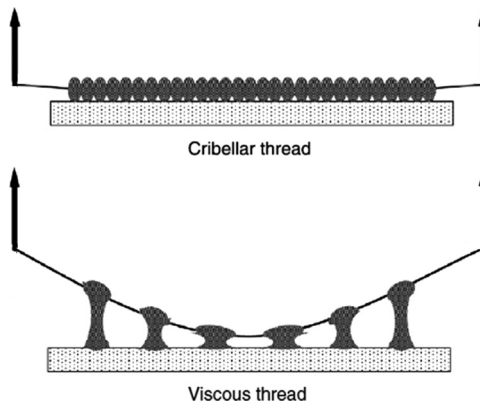

FIGURE 9 Extensibility plays a huge role in adhesion. Figure shows a schematic of the difference in the thread adhesion behavior when a cribellar thread and a viscid thread are detached from a surface. The difference in the axial silk extensibility in both the cases can be attributed partly to this effect. It is adapted from [42] with permission from Springer.

conditions). We, by employing a novel experimental technique, measured the adhesive force of a single glue droplet. Capture silk threads were immobilized on a glass substrate and a conical glass micro-probe was brought into contact with glue droplets. The probe was then retracted at constant controlled speeds while the force was recorded as a function of distance. After reaching the critical pull-off force, the tip releases contact. The force–distance response is highly dependent on the rate of pull-off. Pull-off forces increase from 60 μN at a rate of 1 μm s to around 400 μN at 100 μm s (Fig. 10a). The pull-off forces are many orders of magnitude higher than what we expect for capillary forces and confirm that the glycoprotein, rather than the viscous coat, is responsible for adhesion.

The force relaxation experiments, after stretching the glue droplets by 100 μm, reveal that the forces relax to a constant value that is independent of the rate of displacement. The steady state forces, which are two orders of magnitude higher than those expected for capillary forces, clearly indicate that the glue is responding neither as a viscous liquid nor as a viscoelastic liquid. Instead, the glue exhibits characteristics of a viscoelastic solid (Fig. 10b). This is consistent with the microscopy images of a glycoprotein granule (and the whole glue drop) swelling in water while retaining its shape at high humidity. Furthermore, the elastic response and the absence of terminal
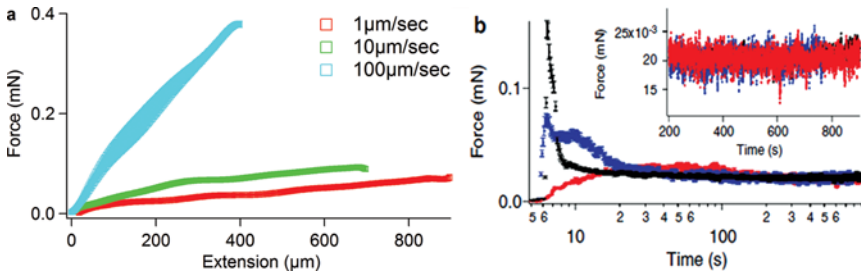

FIGURE 10 Single glue drop adhesion measurements. (a) Force responses when single glue drops were stretched at different rates until separation from a glass probe. Curves are plotted as mean ± s.d. from three measurements each (error bars are in black for all three cases). It is adapted from [40]. (b) Load-relaxation curves in which glue drops were stretched by 100 μm at three different rates [100 μm s (black), 10 μm s (blue), 1 μm s (red)], after which the load was allowed to relax. Inset shows an enlarged view of the plateau regions for the three cases. All measurements were taken close to 25°C at 40% relative humidity (RH). The curves are plotted as mean ± s.d. from three measurements each. It is adapted from [43] (color figure provided online).

flow regions indicate that the glycoproteins are physically or chemically cross-linked.

The elasticity of the glue also plays an important role in how the viscid silk is used by orb-weaving spiders to capture prey. At slow extension rates, similar to the movements of already entangled insects, the glycoproteins deform like an ideal elastic rubber band, which is essential in retaining the insects trapped in the web long enough to be subdued by the spider. At high extension rates, the adhesive forces are dramatically enhanced due to high viscous effects, making it easier for the capture silk threads to hold on to fast flying insects when they initially impact webs. The elegant use of elasticity to enhance adhesive forces occurs in marine mussels and suggests a common design principle in the evolution of natural adhesives.

Viscoelasticity of glue drops has far-reaching consequences on the function of capture threads in spider webs. A single capture thread is covered with many of these glue drops and the peeling of a capture silk thread from a surface depends on both glue drops and the viscoelasticity of silk fibers. The peeling forces of threads from a surface depend on the rate, similar to the results we obtained for the pull-off forces of a single glue droplet (Fig. 11c). Because peeling forces depend on the mechanical properties of both silk fibers and the glue, we need to separate the contributions of each component.

The approach taken to accomplish this was inspired by the treatment taken for rubber adhesion, particularly thin elastic film peeling (Fig. 11a). When the energy theory of fracture is applied to an elastic film peeling from a rigid substrate, the resulting equation for the peel force includes a term depending on the elastic modulus and thickness of the film material. This elastic term, tending to decrease the peel force, is usually negligible. However, under certain circumstances, this term may become very significant, particularly as the peel angle approaches zero. There are three contributions to the energy change: a surface energy term due to the creation of new surfaces, a potential energy term due to the movement of the applied force (considering the film to be inextensible), and an elastic term due to extension of the film in the direction of the applied force. Parallel to this approach, we developed an energy model. The work performed to pull a silk thread off of a surface is consumed in stretching of the axial silk and the energy required to peel glue droplets from the surface. The total work on the system (W_T) is calculated by integrating the product of the force, $f(h)$, times the infinitesimal height change, dh, from h to $h + dh$:

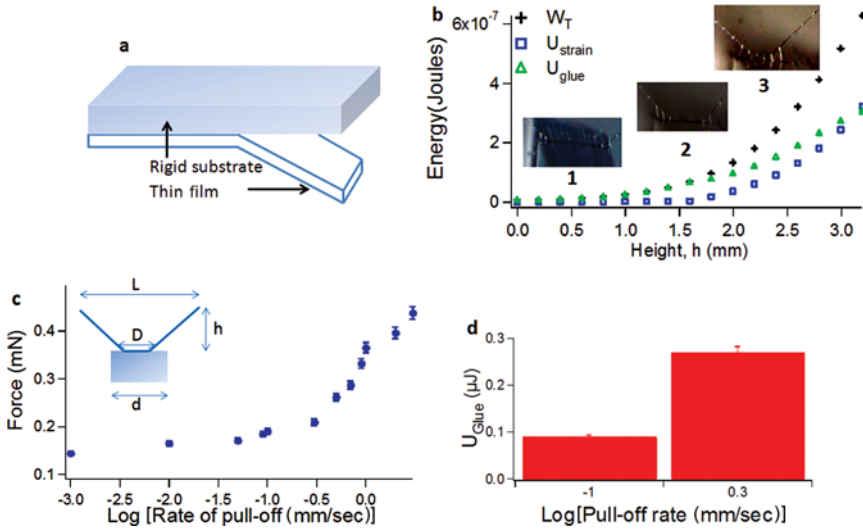$$W_T = \int_{h=0}^{hf} f(h)dh. \tag{1}$$

FIGURE 11 Model to separate the adhesive energy from the strain energy stored in silk fibers. (a) Schematic of a thin-film film peeling measurement. (b) The total work (cross) carried out in separating the thread from the surface, strain energy stored in the axial silk (square), and the energy contribution of the glue drops (triangle) when the thread went through the consecutive stages shown as insets 1, 2, and 3. Calculation of U_{strain} and U_{glue} involved the reasonable approximation that $D \ll L$. In these experiments, this condition is satisfied ($0\,\text{mm} \leq D \leq 2\,\text{mm}$ and $L = 16\,\text{mm}$). The final values of U_{strain} and U_{glue} do not depend on the condition that $D \ll L$. (c) The geometry used for the pull-off measurements is shown in inset. The effect of the rate of pull-off (dh/dt) on the force at pull-off. Values are plotted as mean $\pm$ s.d. from 15 measurements each. (d) Adhesion energies at two pull-off rates using the model explained in the text. It is adapted from [43]. Measurements for Figs. 10 and 11 were performed on the NANO Bionix$^{\text{TM}}$ testing system (MTS; now owned by Agilent Technologies Oak Ridge, TN, USA.) (color figure provided online).

The strain energy stored in the thread when it is pulled from its initial position until it separates from the surface, U_{strain}, is given by the following equation:

$$U_{\text{strain}} = \left(\int_{\varepsilon=0}^{\varepsilon\, at\, pull-off} \sigma(\varepsilon)d\varepsilon \right) * \pi^* r^{2*}(L - D). \qquad (2)$$

$\sigma(\varepsilon)$ is the value of stress at strain ε, and r is the radius of the thread, and h_f is the value of h at pull-off. Stress-strain characteristics of the

silk thread depend on rate of deformation. Subtracting Eq. (2) from Eq. (1) gives the energy required to separate the glue drops from the surface, U_{glue}. The values of U_{glue} depend on intermolecular adhesion as well as on the energy required to stretch the glue droplets (Fig. 11b). Interestingly, these capture fibers, when detaching from a substrate at different rates, stretch in the elastic region such that Eq. (2), without any loss in precision, can be re-written as follows:

$$U_{strain} = \sigma * \varepsilon * V/2 = E * V * \varepsilon^2/2. \qquad (3)$$

This implies that

$$U_{glue} = W_T - U_{strain} = \int_{h=0}^{hf} f(h)dh - E * V * (\sec\theta - 1)^2/2, \qquad (4)$$

where E is the elastic modulus of the thread, and V is the volume of the thread, as explained in Eq. (2), and $\tan\theta = 2 * h_f/L$.

The energies obtained using this model matched with those obtained from the single droplet measurement data and the model is a very useful tool to study the behavior of glue droplets under different conditions [43] (Fig. 11d). As can be observed in Fig. 11b, almost 50% of the energy required to detach a viscid capture silk from a surface is contributed by the axial silk fiber. This contribution varies with parameters such as relative humidity, temperature, and the rate of peeling. Developing this model decouples the axial silk contribution from that of the glue and can help determine the effect of various parameters on both the adhesion of glue droplets and the mechanical properties of the axial silk fibers. This model, with appropriate modifications, can also give valuable insights into other systems such as the bolas silk, sticky gum-footed lines, or the ribbon silk of the brown spider and, thus, has the potential to provide a universal method to understand cause and effect of adhesion in these systems.

3. SUMMARY

Spiders use a diverse variety of silks in different strategies to capture their prey. These different silk fibers often have unique properties that suit their function in webs. The fibers include, but are not limited to, individual silk lines with large gluey blobs at the end that are thrown at prey (e.g., a "bolas" web), spring-loaded sticky gum-footed lines in cobwebs, and the ribbon-like adhesive silk in brown spiders. Cribellar silk and viscid silk are among the most common adhesive threads produced by spiders and comprise the capture spirals of orb webs. In both silks, spiders use elasticity of axial fibers synergistically

with a surrounding adhesive to increase their effectiveness. The study of the chemistry and processes used by spiders and other biological species will provide many insightful strategies of designing new adhesives.

ACKNOWLEDGMENTS

REFERENCES

[1] Yurdumakan, B., Raravikar, N. R., Ajayan, P. M., and Dhinojwala, A., *Chem. Commun.* 3799–3801 (2005).
[2] Lee, H., Lee, B. P., and Messersmith, P. B., *Nature* **448**, 338–342 (2007).
[3] Bond, J. E. and Opell, B. D., *Evolution* **52**, 403–414 (1998).
[4] Shear, W. A., *Spiders, Webs, Behavior, and Evolution* 1st ed., (Stanford University Press, Stanford, 1986), p. 492.
[5] Foelix, R. F., *Biology of Spiders Ch. 5*, 2nd ed., (Oxford University Press, New York, 1996), p. 122.
[6] Blackledge, T. A., Scharff, N., Coddington, J. A., Szuts, T., Wenzel, J. W., Hayashi, C. Y., and Agnarsson, I., *Proc. Nat. Acad. Sci.* **106**, 5229–5234 (2009).
[7] Blackledge, T. A. and Hayashi, C. Y., *J. Exp. Biol.* **209**, 2452–2461 (2006).
[8] Shao, Z. and Vollrath, F., *Nature* **418**, 741 (2002).
[9] Choresh, O., Bayarmagnai, B., and Lewis, R. V., *Biomacromolecules* **10**, 2852–2856 (2009).
[10] Lazaris, A., Arcidiacono, S., Huang, Y., Zhou, J. F., Duguay, F., Chretien, N., Welsh, E. A., Soares, J. W., and Karatzas, C. N., *Science* **295**, 472–476 (2002).
[11] Eberhard, W. G., *Science* **198**, 1173–1175 (1977).
[12] Yeargan, K. V., *Annu. Rev. Entomol.* **39**, 81–99 (1994).
[13] Swanson, D. L. and Vetter, R. S., *Clinics in Dermatology* **24**, 213–221 (2006).
[14] da Silva, P. H., da Silveira, R. B., and Appel, M. H., *Toxicon* **44**, 693–709 (2004).
[15] Knight, D. P. and Vollrath, F., *Phil. Trans. R. Soc. Lond. B* **357**, 219–227 (2002).
[16] Argintean, S., Chen, J., Kim, M., and Moore, A. M. F., *Appl. Phys. A.* **82**, 235–241 (2006).
[17] Blackledge, T. A., Summers, A. P., and Hayashi, C. Y., *Zoology* **108**, 41–46 (2005).
[18] Opell, B. D., *Biol. J. Linnean Soc.* **62**, 443–458 (1997).
[19] Denny, M., *J. Exp. Biol.* **65**, 483–506 (1976).
[20] Opell, B. D., *Biol. J. Linnean Soc.* **68**, 593–612 (1999).
[21] Kullmann, E. J., *Am. Zool.* **12**, 395–405 (1972).
[22] Blackledge, T. A. and Hayashi, C. Y., *J. Exp. Biol.* **209**, 3131–3140 (2006).
[23] Eberhard, W. G. and Pereira, F., *J. Arachnol.* **21**, 161–174 (1993).
[24] Opell, B. D., *Biol. J. Linn. Soc.* **62**, 443–458 (1997).
[25] Opell, B. D., *J. Morphol.* **221**, 111–119 (1994).
[26] Opell, B. D., *J. Morphol.* **224**, 47–56 (1995).
[27] Hawthorn, A. C., *Biol. J. Linn. Soc.* **77**, 1–8 (2002).

[28] Opell, B. D., *Func. Ecol.* **8**, 145–150 (1994).
[29] Opell, B. D., *J. Arachnol.* **17**, 112–114 (1989).
[30] Opell, B. D., *J. Exp. Zool.* **273**, 186–189 (1995).
[31] Hawthorn, A. C. and Opell, B. D., *J. Exp. Biol.* **206**, 3905–3911 (2003).
[32] Opell, B. D., *J. Arachnol.* **25**, 295–306 (1997).
[33] Opell, B. D. and Bond, J. E., *Biol. J. Linn. Soc.* **70**, 107–120 (2000).
[34] Opell, B. D. and Schwend, H. S., *J. Exp. Biol.* **210**, 2352–2360 (2007).
[35] Vollrath, F., Fairbrother, W. J., Williams, R. J. P., Tillinghast, E. K., Bernstein, D. T., Gallagher, K. S., and Townley, M. A. *Nature* **345**, 526–528 (1990).
[36] Edmonds, D. and Vollrath, F., *Proc. R. Soc. Lond.*, **248**, 145–148 (1992).
[37] Tillinghast, E. K. and Sinohara, H., *Biochem. Int.* **9**, 315–317 (1984).
[38] Vollrath, F. and Tillinghast, E. K., *Naturwissenschaften* **78**, 557–559 (1991).
[39] Peters, H. M., *Naturwissenchaften* **82**, 380–382 (1995).
[40] Opell, B. D. and Hendricks, M. L., *J. Exp. Biol.* **213**, 339–346 (2010).
[41] Bonthrone, K. M., Vollrath, F., Hunder, B. K., and Sanders, J. K. M., *Proc. R. Soc. Lond.* **248**, 145–148 (1992).
[42] Opell, B. D. and Hendricks, M. L., *J. Exp. Biol.* **210**, 553–560 (2007).
[43] Sahni, V., Blackledge, T. A., Dhinojwala, A., *Nat. Commun.* **1**, 19 (2010) doi: 10.1038/ncomms1019.